Electronic supplementary information

Nonconventional luminophores with unprecedented efficiencies and color-tunable afterglows

*Yunzhong Wang, Saixing Tang, Yating Wen, Shuyuan Zheng, Bing Yang, and Wang Zhang Yuan**

Y. Wang, S. Tang, S. Zheng, Prof. W. Z. Yuan
School of Chemistry and Chemical Engineering
Frontiers Science Center for Transformative Molecules
Shanghai Key Lab of Electrical Insulation and Thermal Aging
Shanghai Electrochemical Energy Devices Research Center
Shanghai Jiao Tong University
Shanghai 200240, China
E-mail: wzhyuan@sjtu.edu.cn

Y. Wen, Prof. B. Yang
State Key Laboratory of Supramolecular Structure and Materials
College of Chemistry
Jilin University
Changchun 130012, China

Keywords: nonconventional luminophores, persistent room temperature phosphorescence, color-tunable phosphorescence, clustering-triggered emission, through-space conjugation

Experimental section

Materials. Hydantoin (HA) and 5,5-dimethylhydantoin (MHA) were purchased from Aladdin Reagent Co., Ltd. (Aladdin) and recrystallized before use. Formaldehyde (37 wt% in water) and hydrochloric acid (37 wt% in water) were bought from Sinopharm Chemical Reagent Co. Ltd. and used directly. Acetaldehyde (99.5%) was obtained from Aladdin Reagent Co., Ltd. (Aladdin) and used directly. Purified water was provided by Wahaha (Hangzhou) Co., Ltd.

General methods. Element analysis were conducted on an elementary analytical instrument (Vario EL CUBE). ^{1}H and ^{13}C NMR spectra were recorded on a Bruker DRX 500 NMR spectrometer (Germany) using deuterated dimethyl sulfoxide (DMSO-d_6) as solvent at room

temperature. The prompt photoluminescence (PL) spectra, excitation-PL mappings, excitation-phosphorescence mappings (t_d = 0.1 ms) and phosphorescence lifetimes ($<\tau>_p$) for solids were all measured on an Edinburgh FLS1000 photoluminescence spectrometer. The prompt PL spectra of solutions were measured on a Perkin-Elmer LS 55 PL spectrometer. Absorption spectra of crystals and solutions were measured on PerkinElmer Lambda750s and Lambda 35 UV/Vis spectrometer, respectively. Fluorescence lifetimes ($<\tau>_f$) of the samples were measured on QM/TM/IM steady-state & time-resolved fluorescence spectrofluorometer (PTI, USA). The absolute quantum efficiencies (Φ) were measured with an Absolute PL Quantum Yield Spectrometer Quantaurus-QY C11347-11. The single crystal structure determination was performed on a Bruker D8 VENTURE X-ray Diffractometer at room temperature. All photographs and videos were taken by a digital camera (Sony α7sⅡ, Japan). Freeze-drying was performed on a FD-2D freeze dryer (Bilang Instrument Co., Ltd, Shanghai).

Computational Study. The single molecule (monomer), dimer, trimer, and tetramer of HA were extracted from their single crystal data. Time dependent density functional theory (TD-DFT) was used to calculate the excitation energy and transition character using B3LYP hybrid functional and 6-31G* basis set. All TD-DFT calculations were performed within Gaussian 09 (version 9.5) program.

Purification and synthesis. HA and MHA solids were first recrystallized and then were utilized for the cultivation of single crystals suitable for X-ray crystallography. MDHA and EDHA were synthesized according to Scheme S1. Their detailed synthesis and purification procedures are described below. **Note:** Samples utilized for measurements or for preparing the solutions are from the corresponding single crystals unless specified.

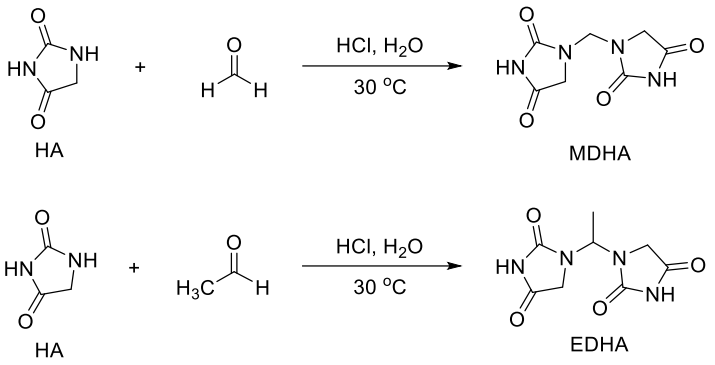

Scheme S1. Synthetic routes to MDHA and EDHA.

Purification of HA. Recrystallization of HA was performed through slow cooling its hot and saturated aqueous solution. The resulting crystals were collected through filtration and used for further cultivation of single crystals. Single crystals of HA suitable for X-ray crystallography were obtained by slow evaporation of its aqueous dilute solution at 25 °C. ^{1}H NMR (500 MHz, DMSO-d_6) δ (ppm) 10.62 (s, 1H), 7.71 (s, 1H), 3.85 (d, J = 1.1 Hz, 2H). ^{13}C NMR (126 MHz, DMSO-d_6) δ (ppm) 174.33, 158.80, 47.69.

Purification of MHA. Recrystallization of MHA was performed through slow cooling its hot and saturated aqueous solution. Colorless crystals were obtained through filtration, and then were used for further cultivation of single crystals. Single crystals of MHA suitable for X-ray crystallography were obtained by slow evaporation of its aqueous dilute solution at 25 °C. ^{1}H NMR (500 MHz, DMSO-d_6) δ (ppm) 10.55 (s, 1H), 7.94 (d, J = 3.8 Hz, 1H), 1.25 (s, 6H). ^{13}C NMR (126 MHz, DMSO-d_6) δ (ppm) 179.59, 156.39, 59.30, 25.07.

Synthesis of MDHA. HA powders (10.00 g, 0.1 mol) and purified water (10 mL) were placed into a single-necked flask. Then, concentrated hydrochloric acid (15 mL, 37 wt%) was slowly added under stirring. Afterwards, the flask was sealed with a rubber stopper, and aqueous solution of formaldehyde (5.2 mL, 37 wt%) was slowly injected with a syringe. The mixture was stirred at 30 °C for 72 h, and white paste-like solid-liquid mixture was obtained and then separated by

suction filtration using a sand funnel. The obtained cake was washed with a large amount of purified water to obtain a white solid, which was freeze-dried for 3 days to yield a white solid powder (9.81 g). MDHA single crystals suitable for X-ray single crystal crystallography were obtained as colorless needle crystals by slow cooling of its hot aqueous solution. ^{1}H NMR (500 MHz, DMSO-d_6) δ (ppm) 10.87 (s, 2H), 4.74 (s, 2H), 3.94 (s, 4H). ^{13}C NMR (126 MHz, DMSO-d_6) δ (ppm) 172.19, 157.81, 50.49, 48.94.

Synthesis of EDHA. Following the similar procedure to that described above for MDHA, just changing the aqueous formaldehyde solution to acetaldehyde (4.24 mL, 0.08 mol), EDHA was obtained as white powders (8.72 g). EDHA single crystals suitable for X-ray single crystal crystallography were obtained as colorless needle crystals by slow cooling of its hot aqueous solution. ^{1}H NMR (500 MHz, DMSO-d_6) δ (ppm) 10.82 (s, 2H), 5.68 (q, J = 6.9 Hz, 1H), 4.01 (d, J = 7.4 Hz, 4H), 1.45 (d, J = 7.0 Hz, 3H). ^{13}C NMR (126 MHz, DMSO-d_6) δ (ppm) 172.13, 156.60, 56.17, 48.71, 16.92.

The element analysis data (%) for HA, MHA, MDHA and EDHA are listed in Table S1.

Table S1. The element analysis data of HA, MHA, MDHA and EDHA.

Compound	Formula	Items	C [%]	H [%]	N [%]
HA	$C_3H_4N_2O_2$	calcd.	36.01	4.03	27.99
		found	36.26	4.35	28.36
MHA	$C_5H_8N_2O_2$	calcd.	46.87	6.29	21.86
		found	47.04	6.03	22.04
MDHA	$C_7H_8N_4O_4$	calcd.	39.63	3.80	26.41
		found	39.68	4.15	26.44
EDHA	$C_8H_{10}N_4O_4$	calcd.	42.48	4.46	24.77
		found	42.62	4.68	25.13

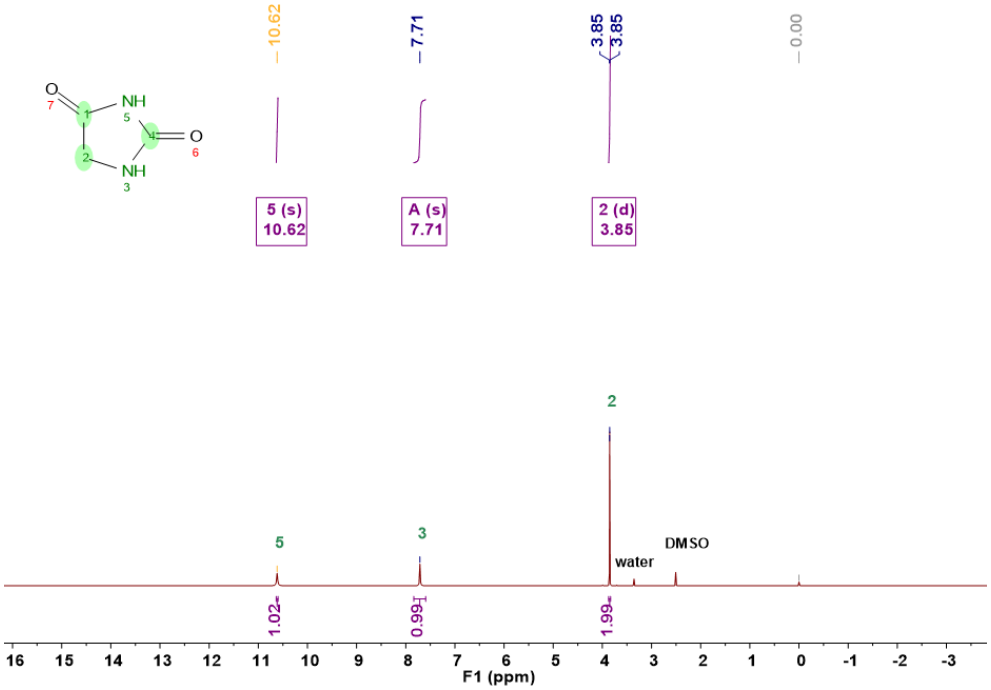

Fig. S1 ^{1}H NMR spectrum of HA in DMSO-d_6.

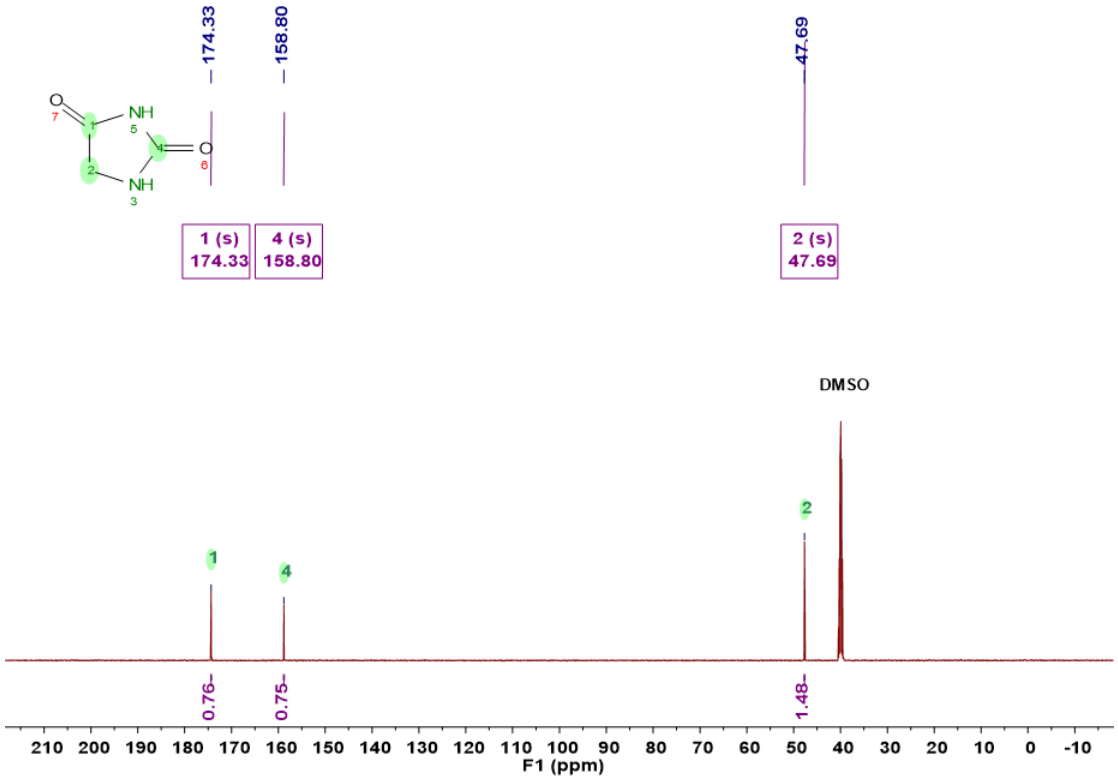

Fig. S2 ^{13}C NMR spectrum of HA in DMSO-d_6.

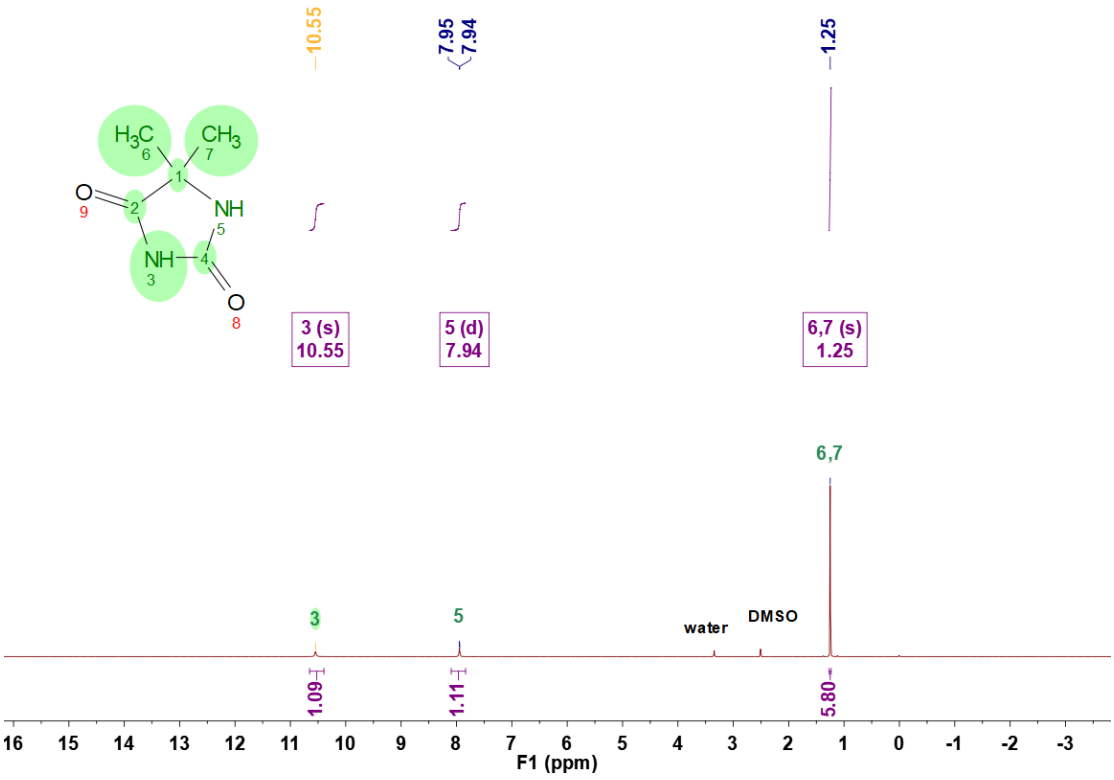

Fig. S3 ^{1}H NMR spectrum of MHA in DMSO-d_6.

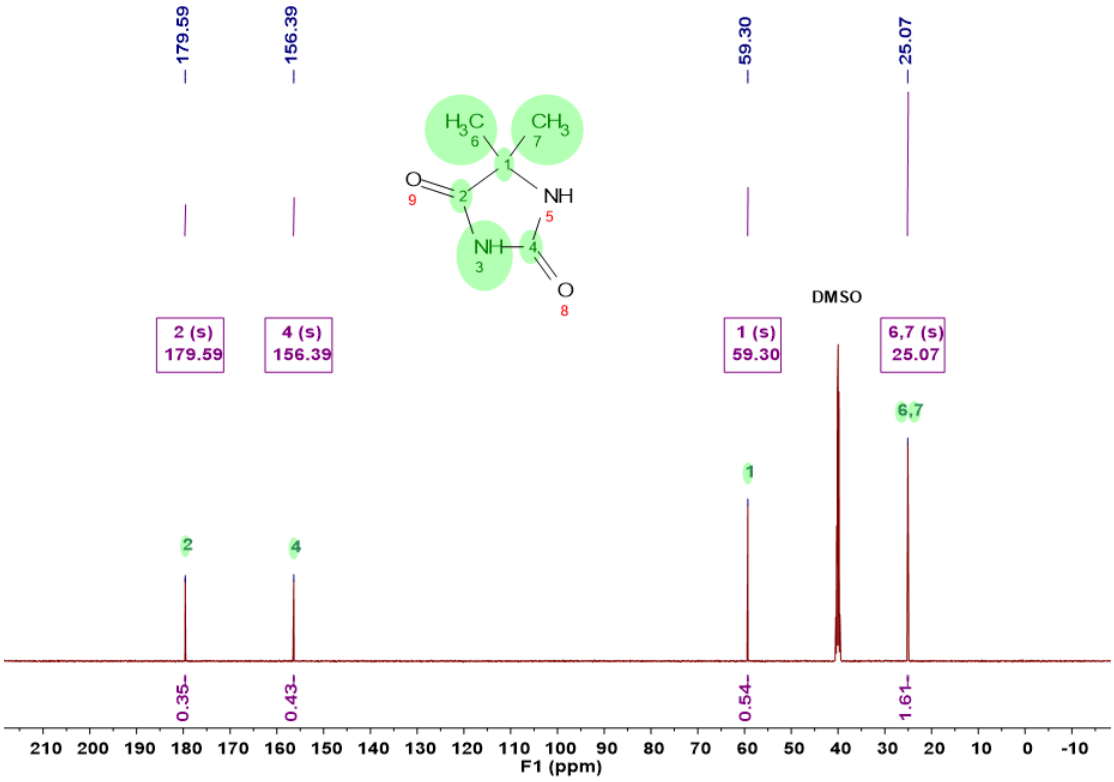

Fig. S4 ^{13}C NMR spectrum of MHA in DMSO-d_6.

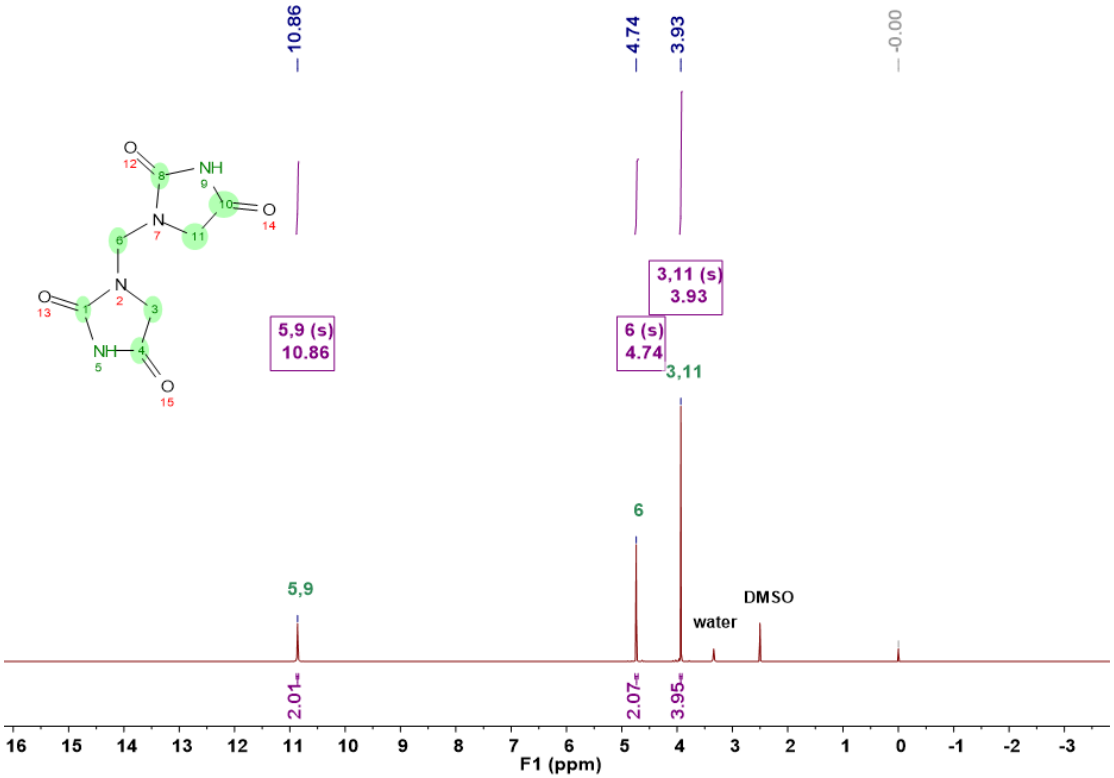

Fig. S5 ^{1}H NMR spectrum of MDHA in DMSO-d_6.

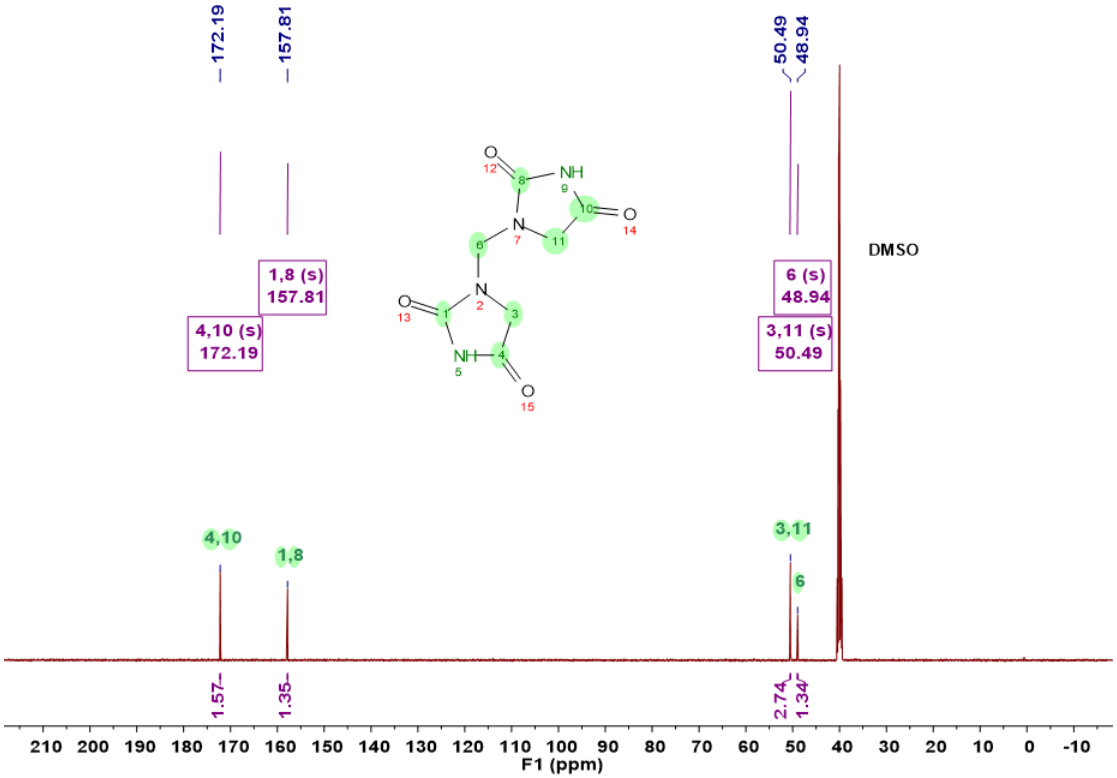

Fig. S6 ^{13}C NMR spectrum of MDHA in DMSO-d_6.

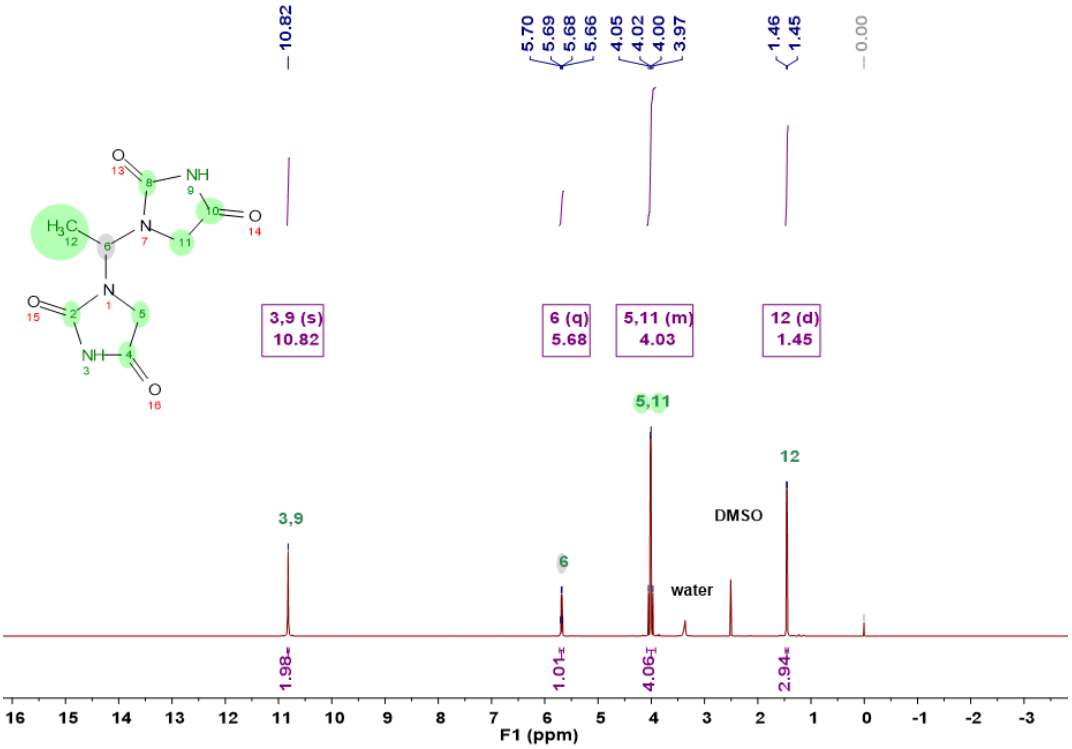

Fig. S7 ^{1}H NMR spectrum of EDHA in DMSO-d_6.

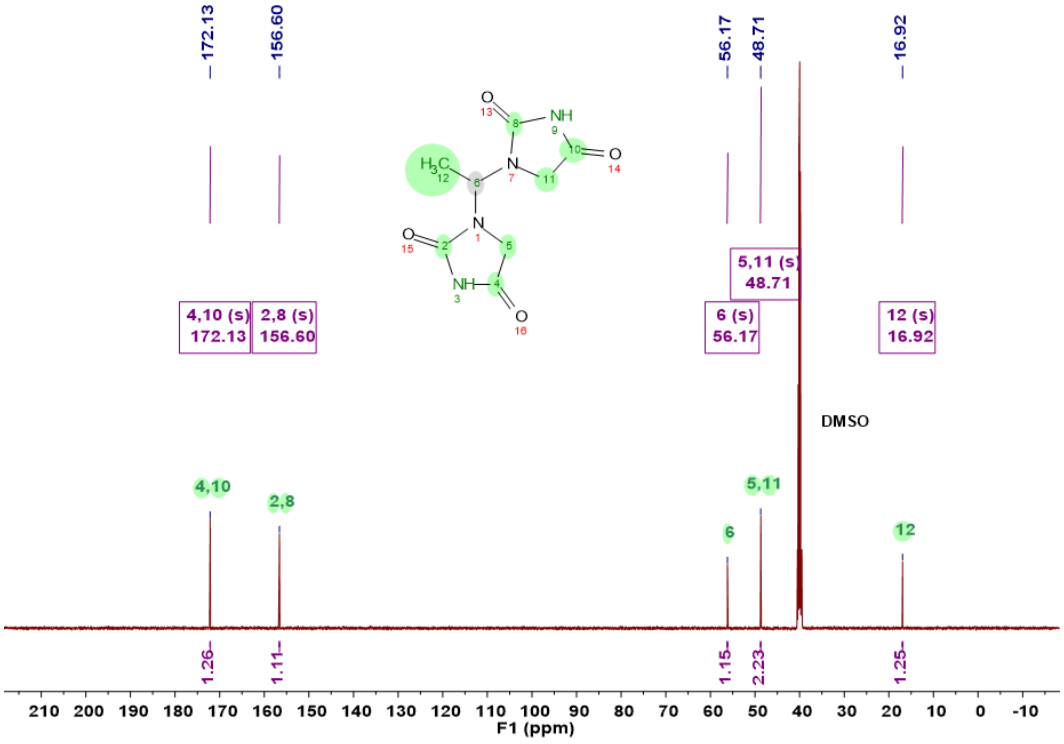

Fig. S8 ^{13}C NMR spectrum of EDHA in DMSO-d_6.

Table S2. Single crystal data of HA, MHA, MDHA and EDHA.

Name	Formula	Space Group	Cell Length [Å]	Cell Angle [°]	Cell Volume [Å^3]	Z	Density [g cm^{-3}]
HA	$C_3H_4N_2O_2$	Monoclinic, C2/c	a = 9.3446 (15) b = 12.244 (2) c = 7.3458 (13)	α = 90 β = 105.194 (7) γ = 90	811.1 (2)	8	1.639
MHA	$C_5H_8N_2O_2$	Orthorhombic, P2(1)2(1)2(1)	a = 7.1989 (6) b = 7.2267 (7) c = 13.0042 (13)	α = 90 β = 90 γ = 90	676.53 (11)	4	1.258
MDHA	$C_7H_8N_4O_4$	Monoclinic, P2(1)/n	a = 9.597 (3) b = 17.769 (5) c = 11.340 (4)	α = 90 β = 114.24 (4) γ = 90	1763.2 (11)	8	1.599
EDHA	$C_8H_{10}N_4O_4$	Monoclinic, P2(1)/c	a = 5.8982 (5) b = 12.4995 (11) c = 14.3372 (10)	α = 90 β = 114.292 (3) γ = 90	963.42 (14)	4	1.560

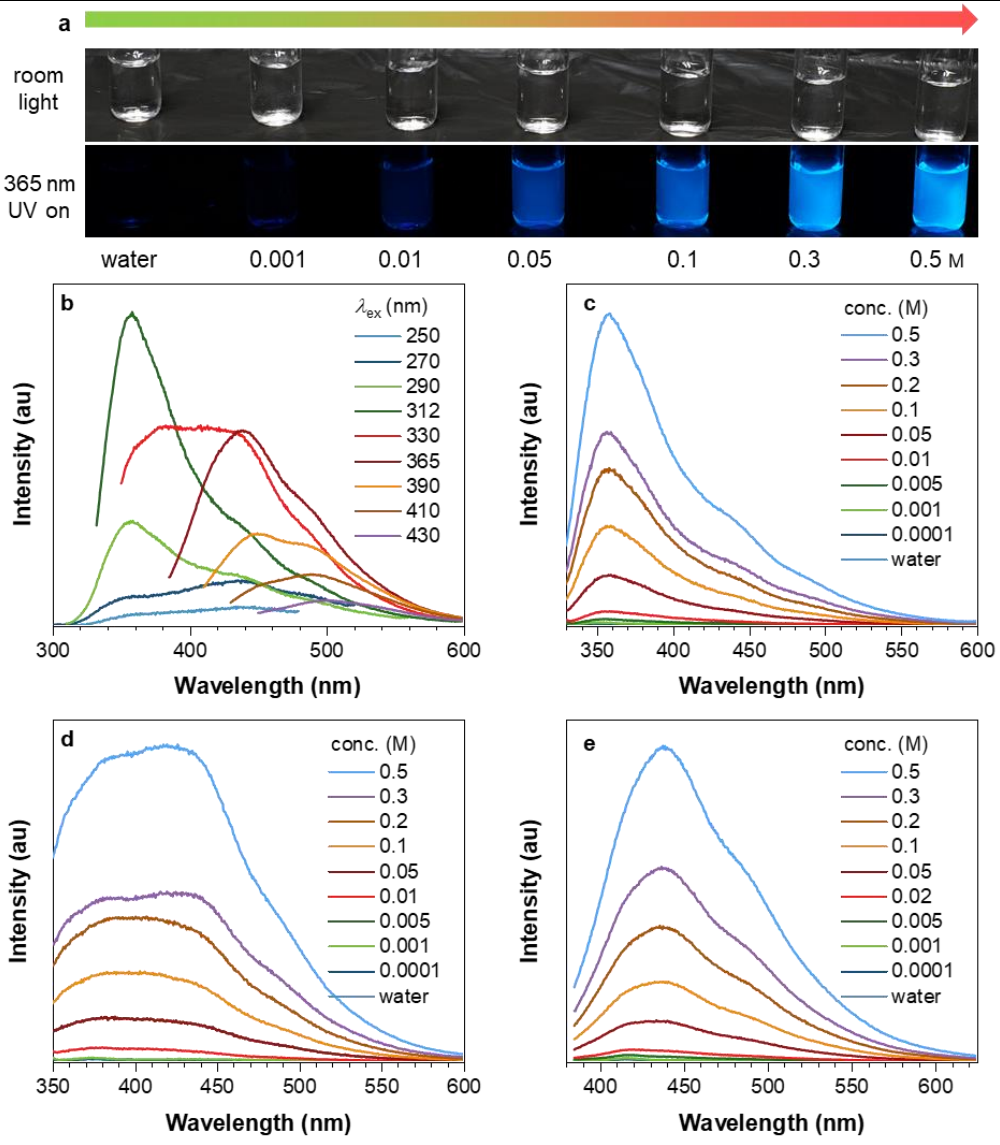

Fig. S9 a, Photographs of different aqueous solutions of HA under room light and 365 nm UV light. **b**, PL spectra of 0.5 M aqueous HA solution at different excitation wavelengths (λ_{ex}s). **c**–**e**, PL spectra of different aqueous solutions of HA with λ_{ex}s of (**c**) 312, (**d**) 330 and (**e**) 365 nm.

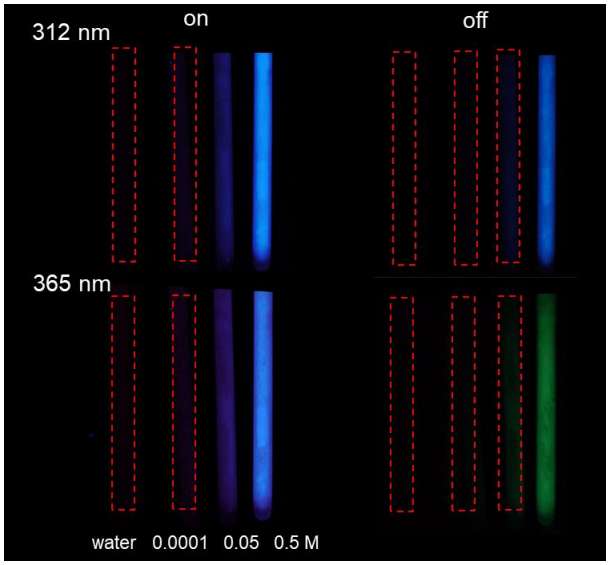

Fig. S10 Photographs of varying aqueous HA solutions taken before and after ceasing different UV excitations at 77 K.

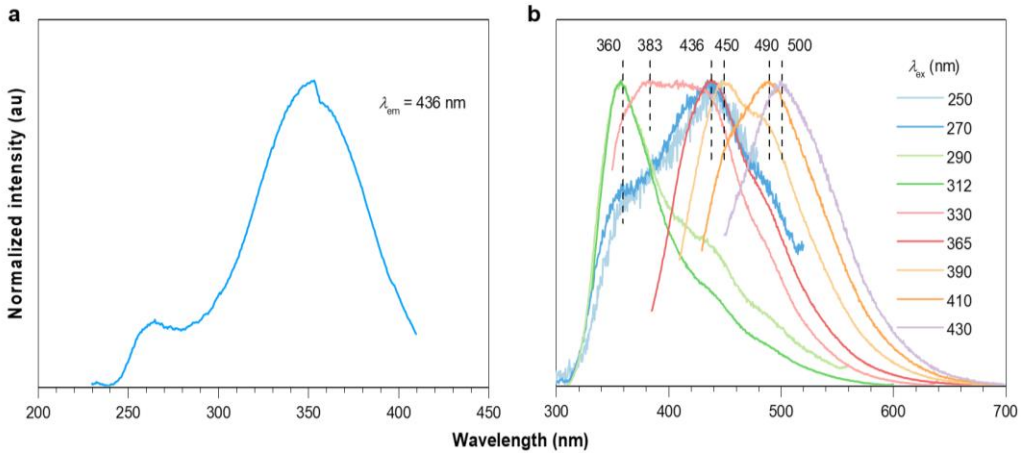

Fig. S11 a, Normalized excitation and **b**, emission spectra of 0.5 M aqueous HA solution.

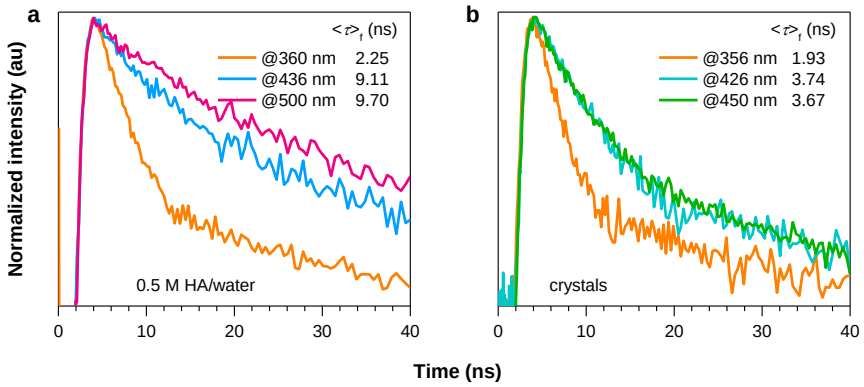

Fig. S12 a,**b**, Time-resolved decay profiles of fluorescence from (**a**) 0.5 M aqueous solution and (**b**) crystals of HA monitored at different wavelengths (λ_{ex} = 330 nm).

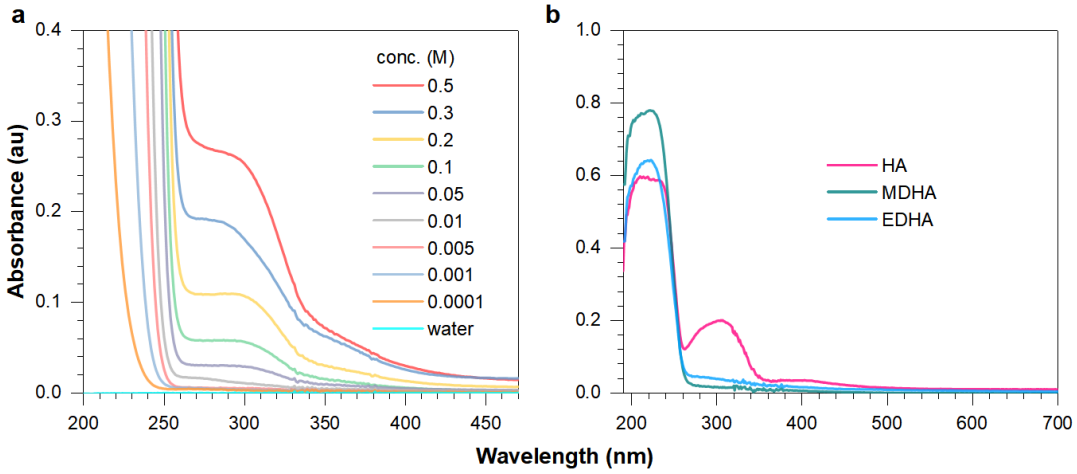

Fig. S13 a,**b**, Absorption of (**a**) varying aqueous HA solutions and (**b**) HA, MDHA and EDHA crystals.

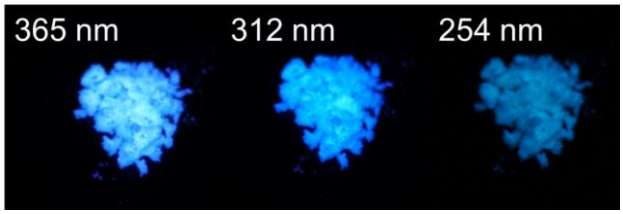

Fig. S14 Photographs of HA crystals taken under different UV lights as indicated.

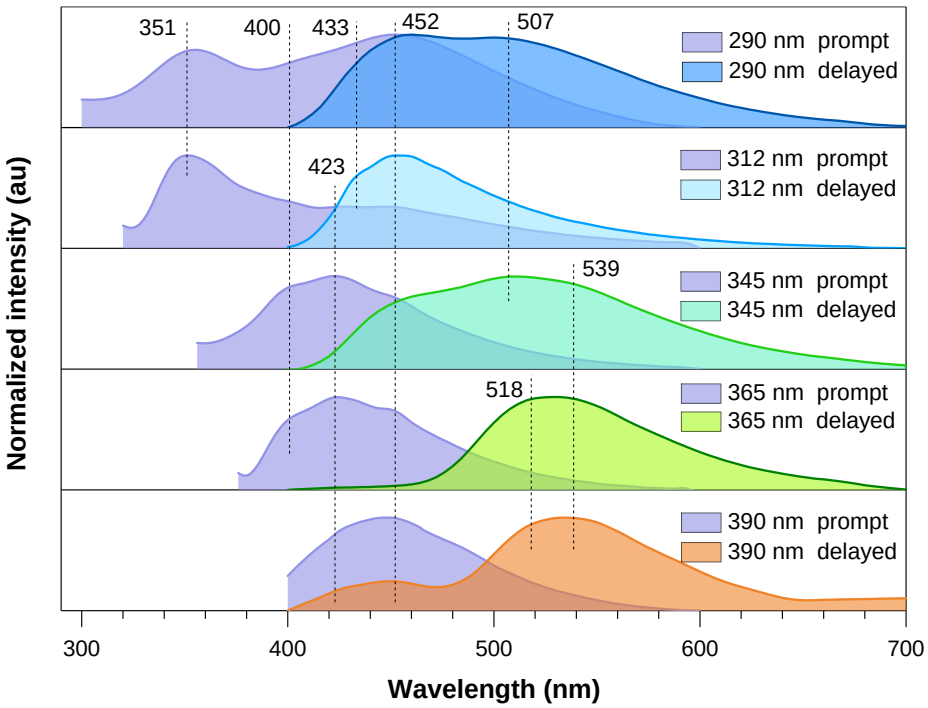

Fig. S15 Normalized prompt and delayed emission spectra of HA crystals under different λ_{ex}s.

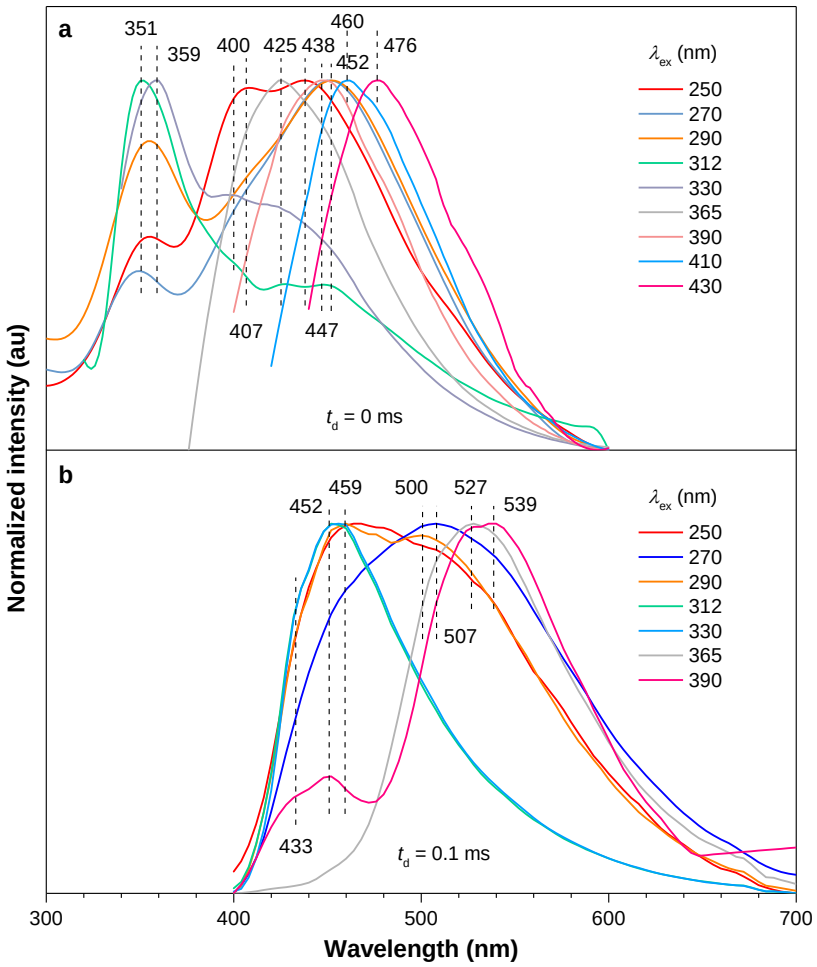

Fig. S16 a,**b**, Normalized (**a**) prompt and (**b**) delayed emission spectra of HA crystals with different λ_{ex}s.

Table S3. p-RTP lifetimes of varying crystals.

Compound	λ_{ex} [nm]	λ_{em} [nm]	$<\tau>_1$ [ms]	$<\tau>_2$ [ms]	$<\tau>_3$ [ms]	B_1 [%]	B_2 [%]	B_3 [%]	χ^2	$<\tau>$ [ms]
HA	312	456	43.8	360.7	1539.5	8.22	25.75	66.03	1.298	1113.0
	365	528	68.1	314.0	1741.6	10.26	15.68	74.06	1.250	1346.0
MDHA	312	450	36.7	312.1	1270.2	6.46	27.39	66.16	1.184	928.2
	365	535	63.8	758.1	--	19.70	80.30	--	1.626	621.3
EDHA	280	510	16.1	128.7	907.5	29.37	27.29	43.34	1.207	433.1
	312	450	100.6	673.0	--	31.70	68.30	--	1.489	491.5
	365	550	17.5	132.8	733.1	14.41	33.43	52.16	1.296	429.3

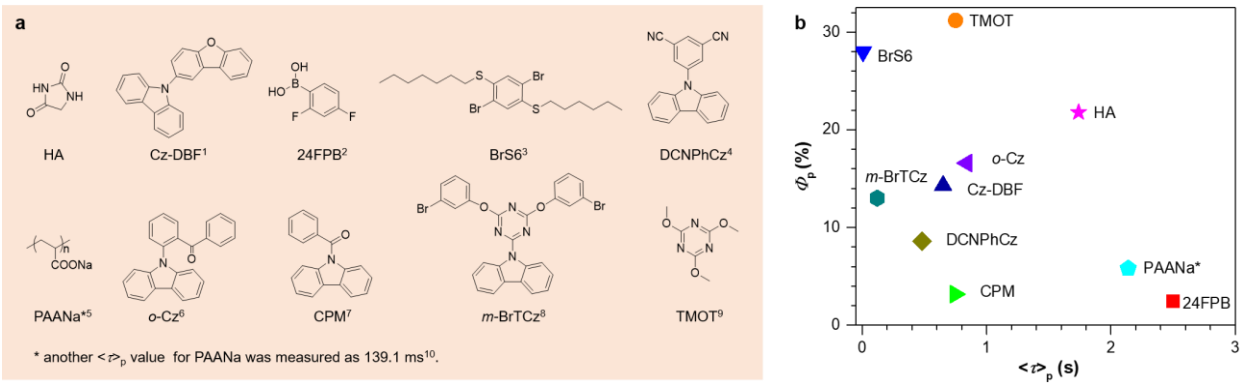

Fig. S17 a, Chemical structures of different luminophores and **b**, their corresponding Φ_p and $<\tau>_p$ values[1-10].

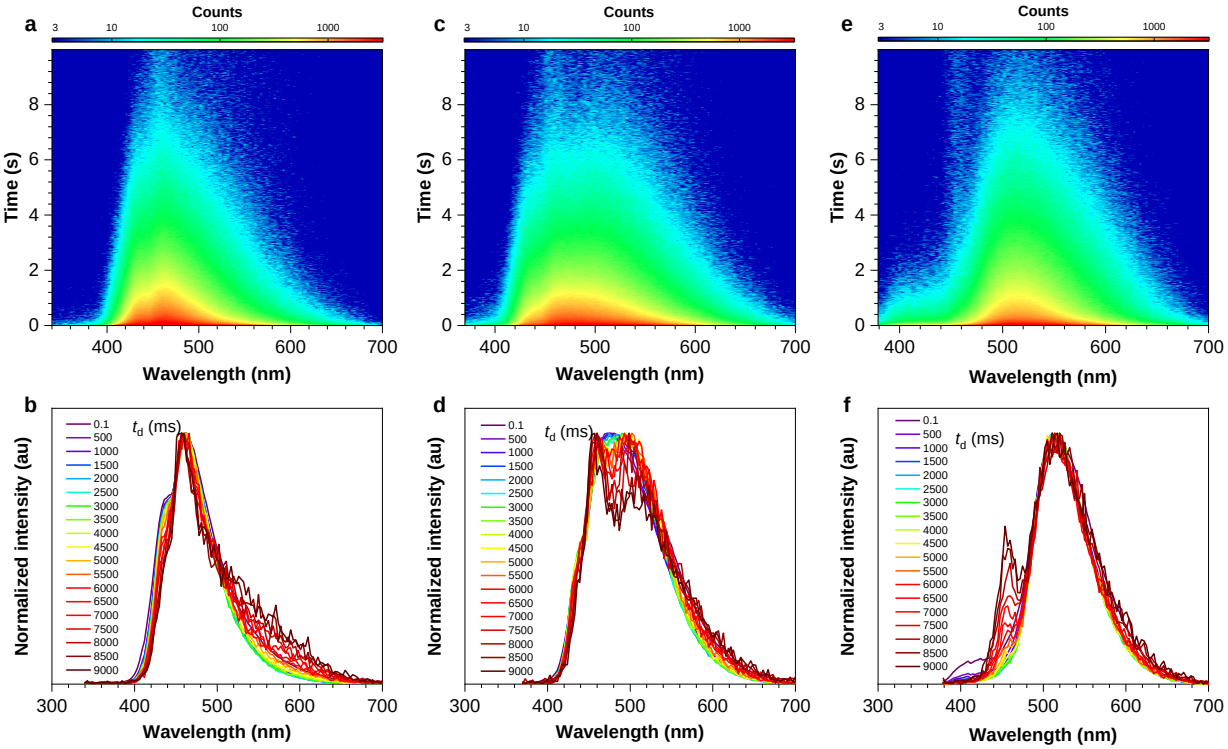

Fig. S18 Time-resolved emission spectra (TRES) of HA crystals under (**a**) 312, (**c**) 345 and (**e**) 365 nm excitations at room temperature. p-RTP emission spectra of HA crystals at different delayed time (from 0.1 to 9000 ms) under (**b**) 312, (**d**) 345 and (**f**) 365 nm excitations.

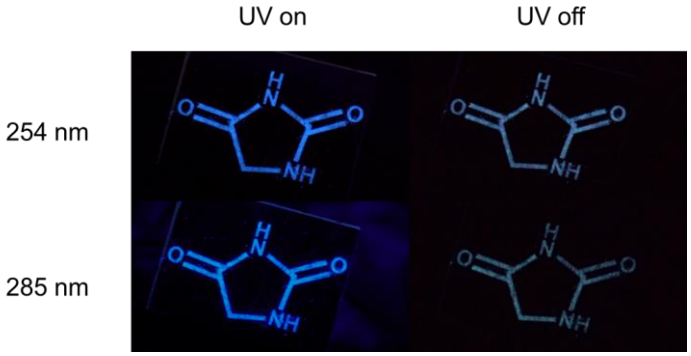

Fig. S19 Photographs of anticounterfeiting patterns based on HA crystals taken under 254 and 285 nm or after ceasing the irradiations.

Table S4. Dynamic photophysical parameters of varying compounds at room temperature.[a)]

Compound	λ_{ex} [nm]	Φ [%]	Φ_f [%]	Φ_p [%]	$<\tau>_p$ [ms]	k_r^p [s^{-1}]	$k_{nr}^p + k_q^p$ [s^{-1}]
HA	312	5.3	2.2	3.1	1539.5	0.02	0.63
	365	87.5	65.7	21.8	1741.6	0.13	0.45
MDHA	312	3.3	2.2	1.1	1270.2	0.01	0.78
	365	17.0	13.4	3.6	758.1	0.05	1.27
EDHA	365	7.3	5.0	2.3	733.1	0.03	1.33

[a)] $<\tau>_p$ is the longest component adopted from the lifetime measurement. $k_r^p = \Phi_p/<\tau>_p$, $k_{nr}^p + k_q^p = (1-\Phi_p)/<\tau>_p$.

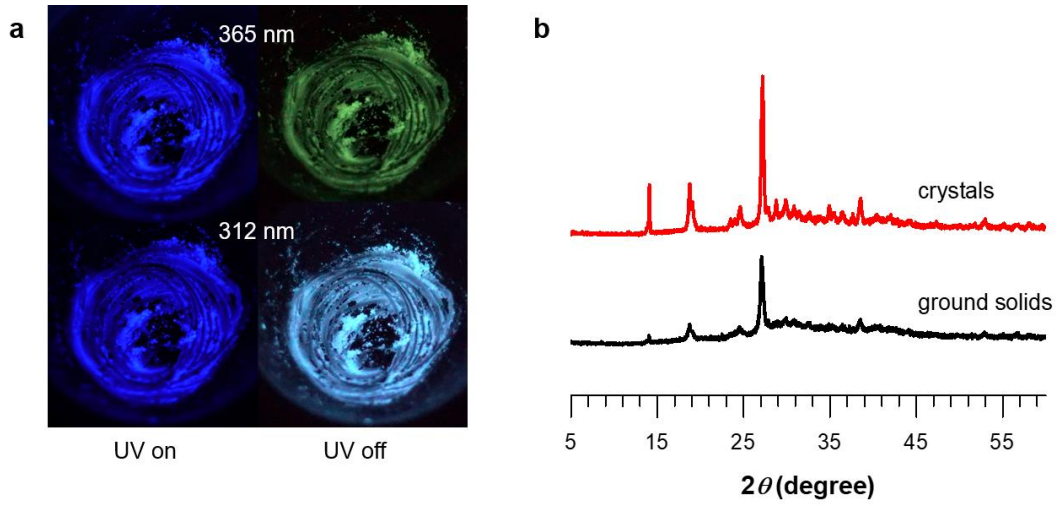

Fig. S20 a, Photographs of ground HA solids taken before and after ceasing different UV excitations. **b**, Power XRD patterns of HA crystals and the ground solids.

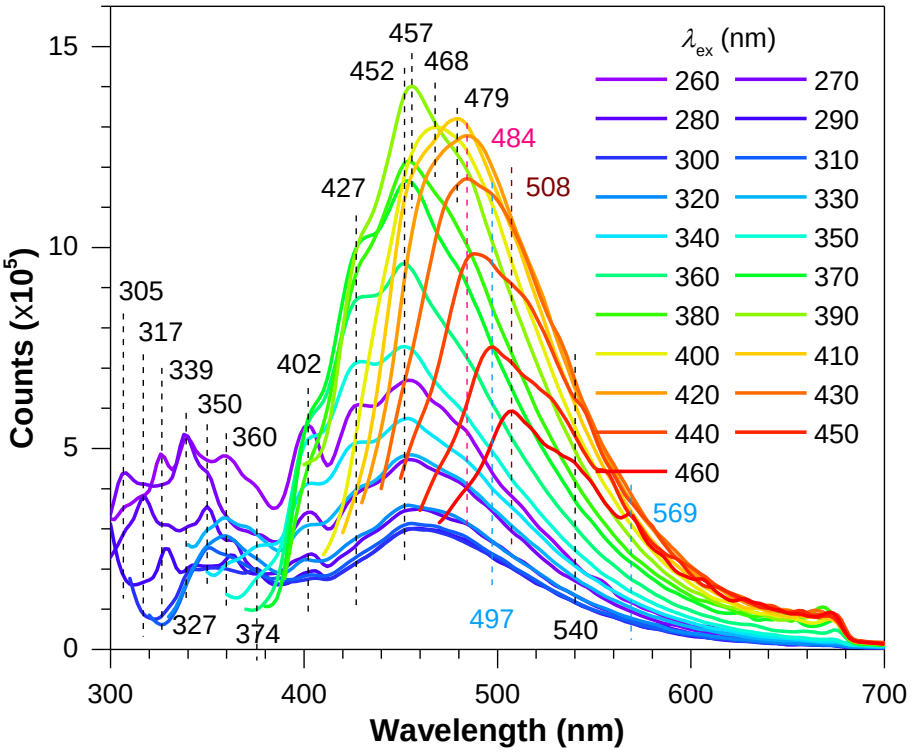

Fig. S21 PL spectra of HA crystals with different λ_{ex}s at 77 K.

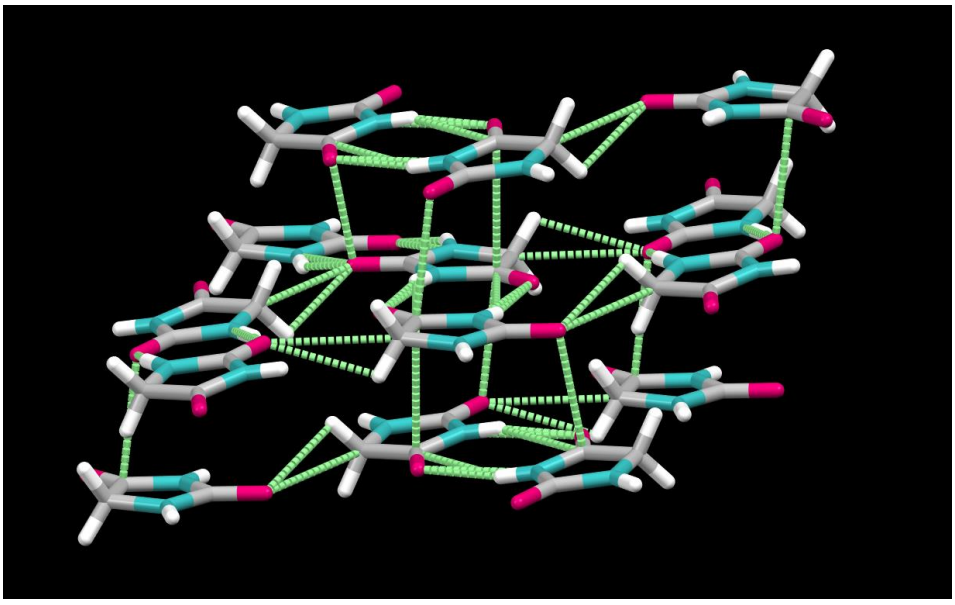

Fig. S22 Fragmental molecular packing and intermolecular interactions of HA crystals.

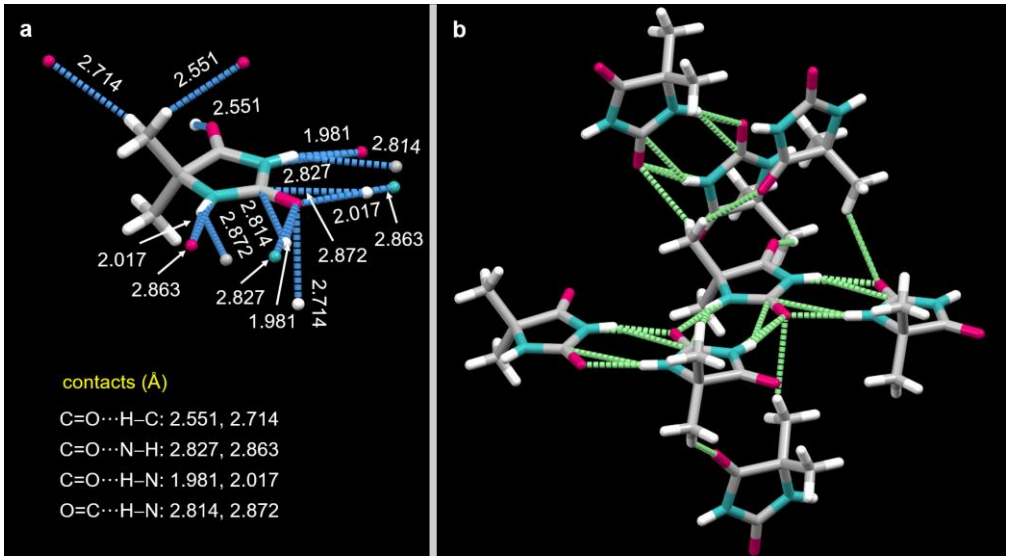

Fig. S23 a, Crystal structure and intermolecular interactions around one molecule in of MHA crystals. **b**, Fragmental molecular packing and intermolecular interactions of MHA crystals.

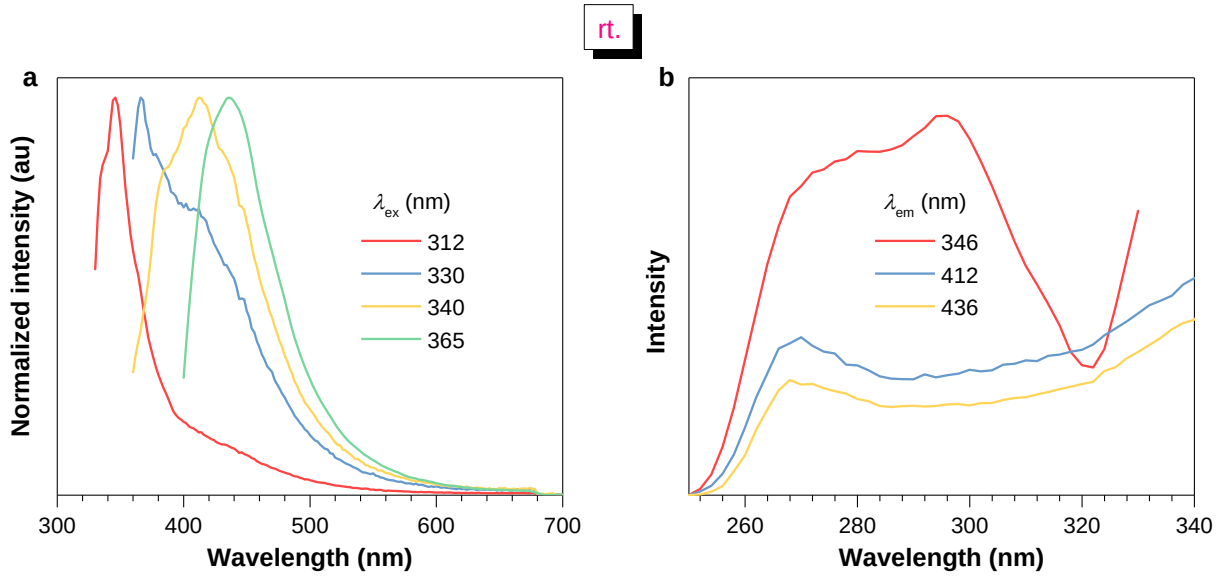

Fig. S24 a, Normalized emission spectra and **b**, excitation spectra of MHA crystals with different (**a**) λ_{ex}s and (**b**) λ_{em}s at room temperature (rt.).

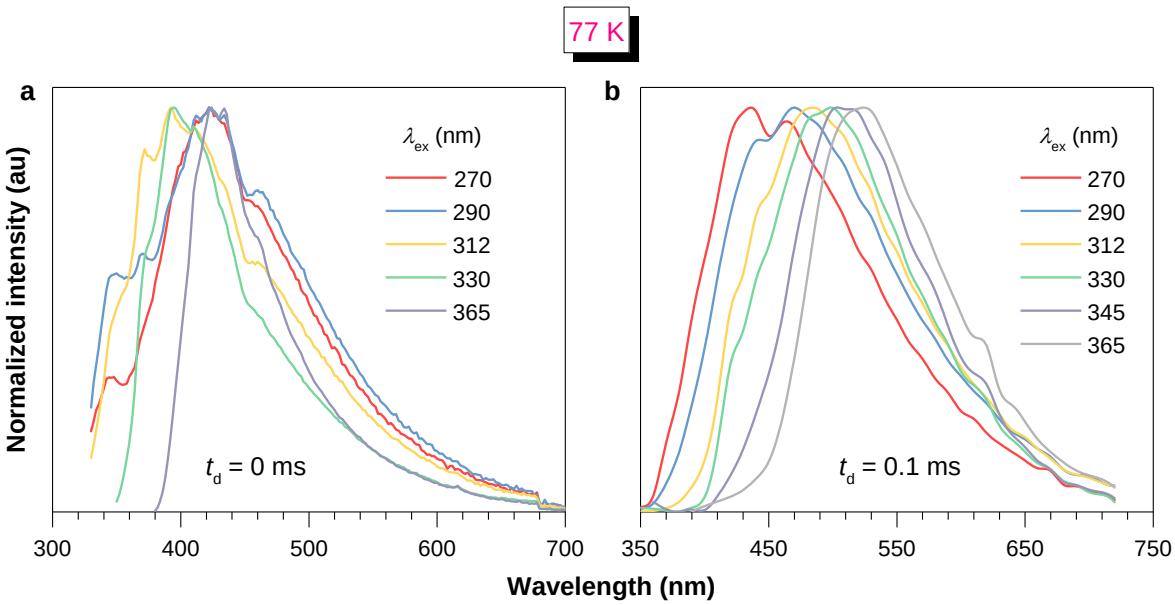

Fig. S25 a,**b**, Normalized (**a**) prompt (t_d = 0 ms) and (**b**) delayed (t_d = 0.1 ms) emission spectra of MHA crystals with different λ_{ex}s at 77 K.

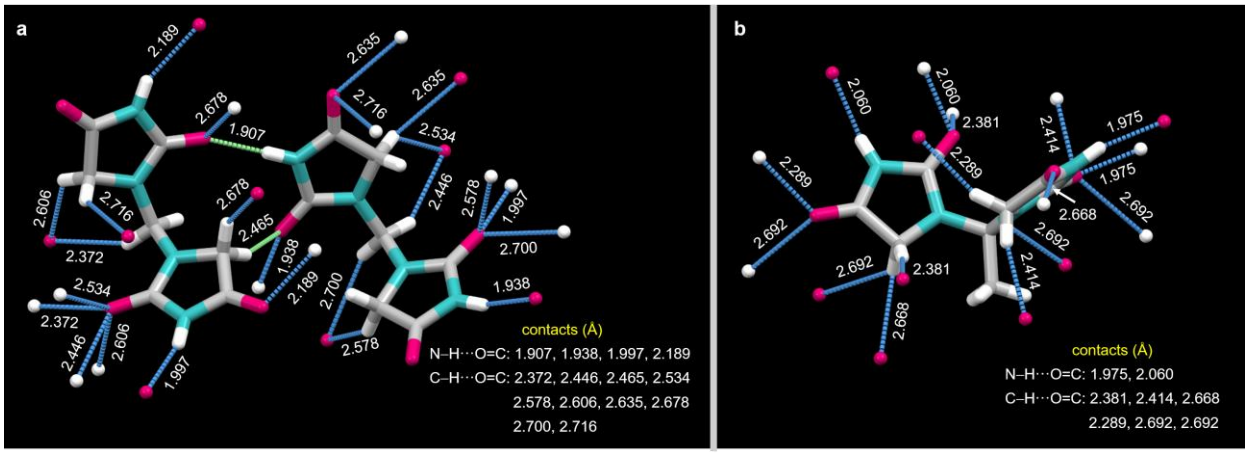

Fig. S26 a,**b**, Single crystal structure of (**a**) MDHA and (**b**) EDHA with denoted N–H···O and C–H···O intermolecular interactions around the molecules.

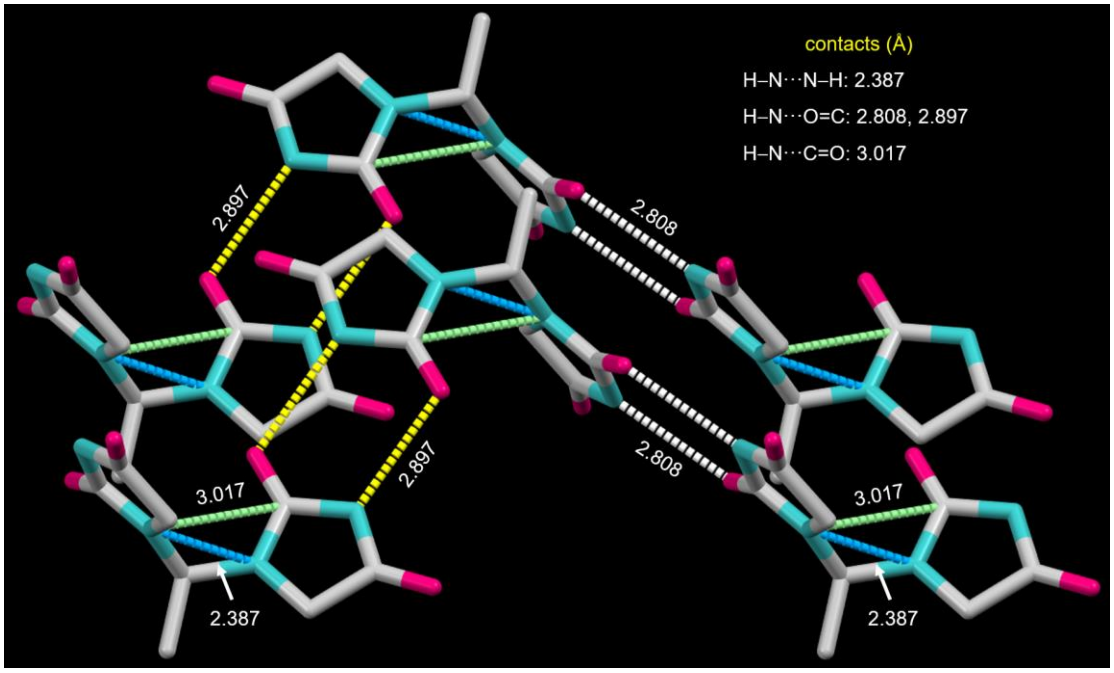

Fig. S27 Fragmental molecular packing of EDHA crystals with 3D through-space conjugation.

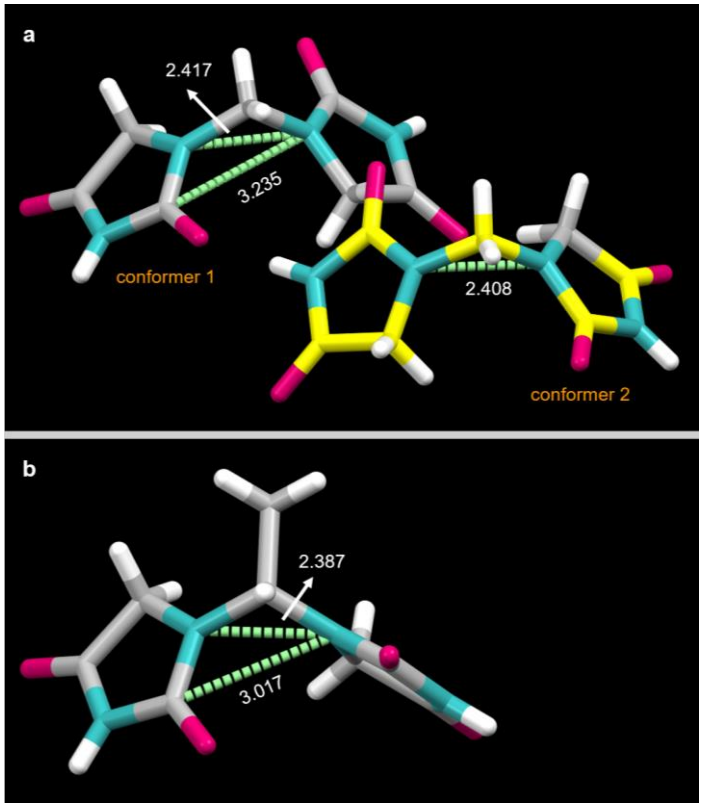

Fig. S28 a,**b**, Crystal structures with denoted intramolecular through-space conjugations for (**a**) MDHA and (**b**) EDHA.

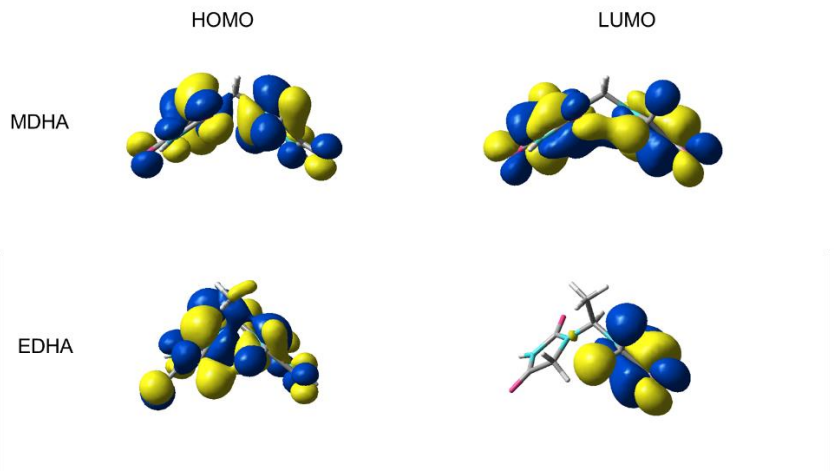

Fig. S29 Electron densities of HOMO and LUMO levels for MDHA and EDHA.

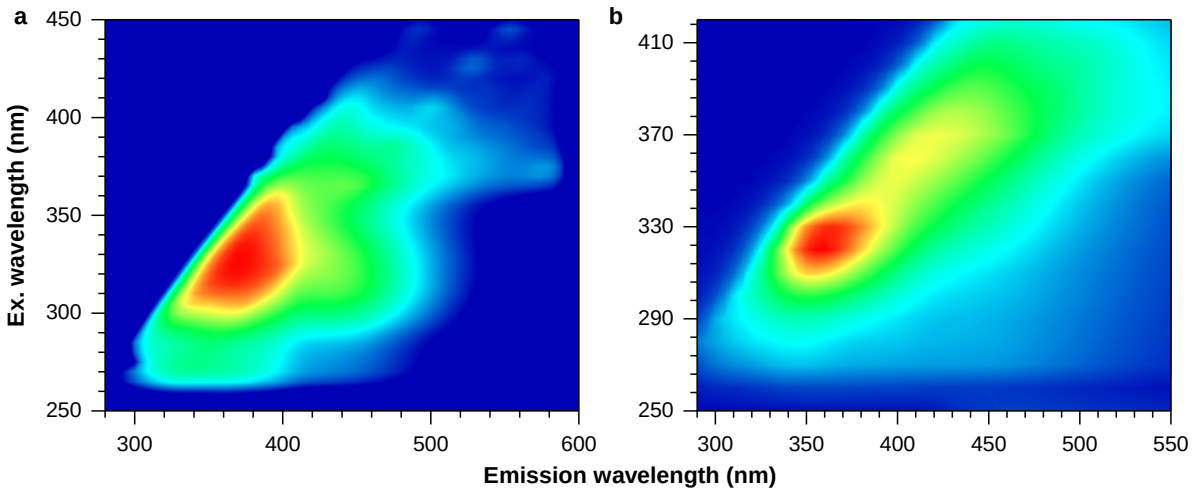

Fig. S30 a,**b**, Excitation-PL mappings of (**a**) MDHA and (**b**) EDHA crystals at room temperature.

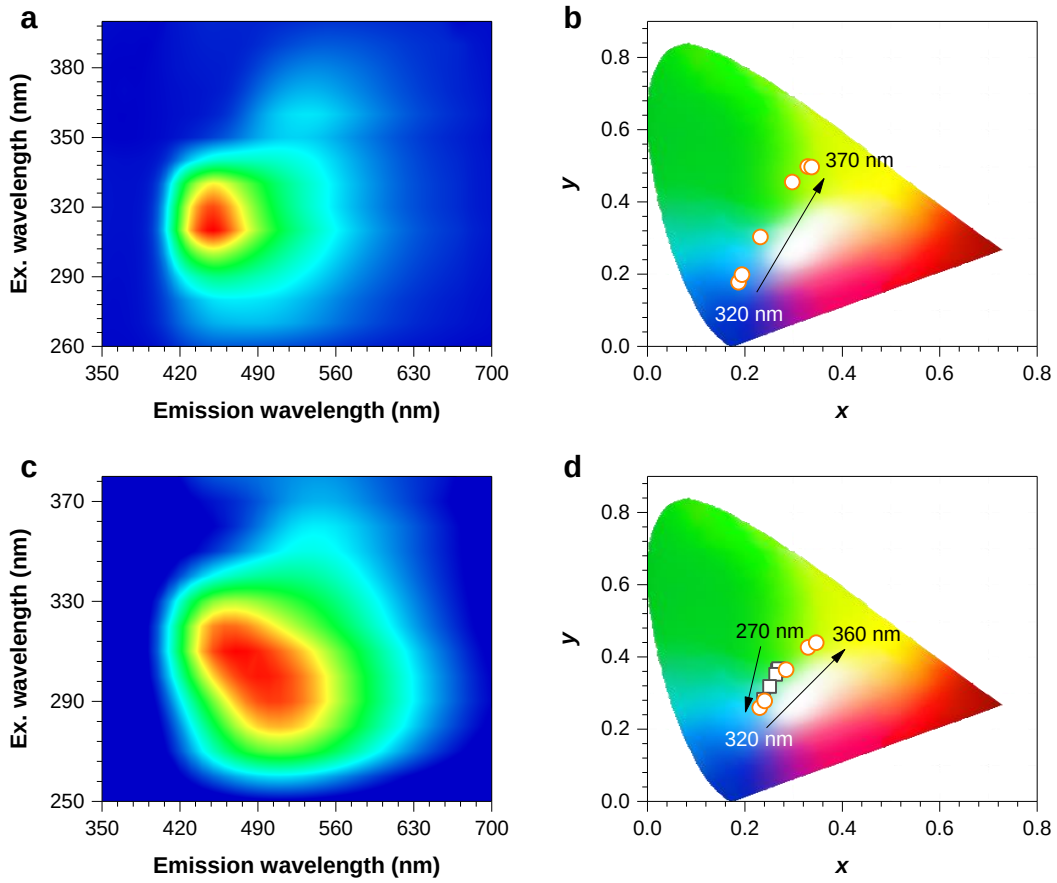

Fig. S31 a,**c**, Excitation-phosphorescence mapping of (**a**) MDHA and (**c**) EDHA crystals (t_d = 0.1 ms). **b**,**d** The CIE coordinate diagrams exhibiting the phosphorescence color variation of (**b**) MDHA and (**d**) EDHA crystals with changing λ_{ex}s.

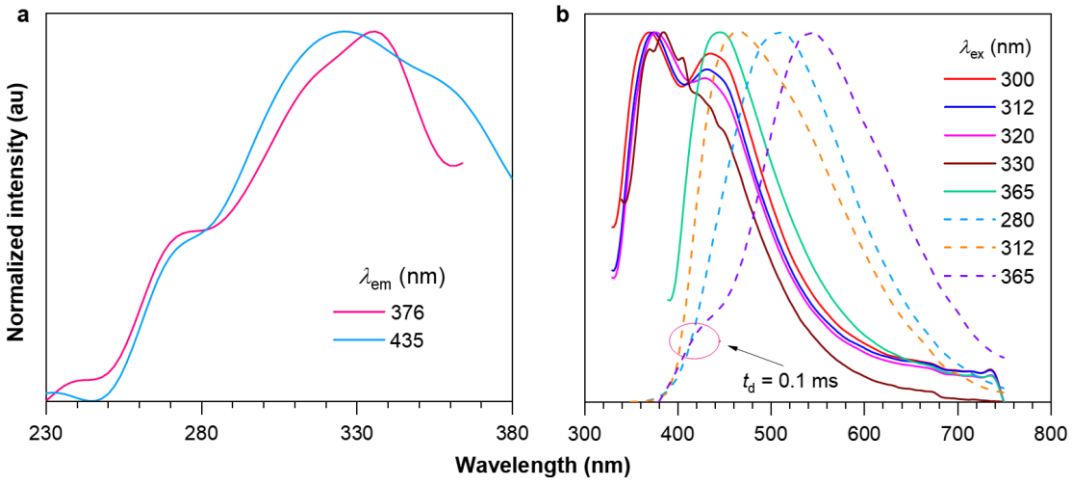

Fig. S32 a, Excitation spectra of EDHA crystals with λ_{em}s of 376 and 435 nm. **b**, Prompt (solid lines) and delayed (dash lines) emission spectra of EDHA crystals upon excitation of different λ_{ex}s.

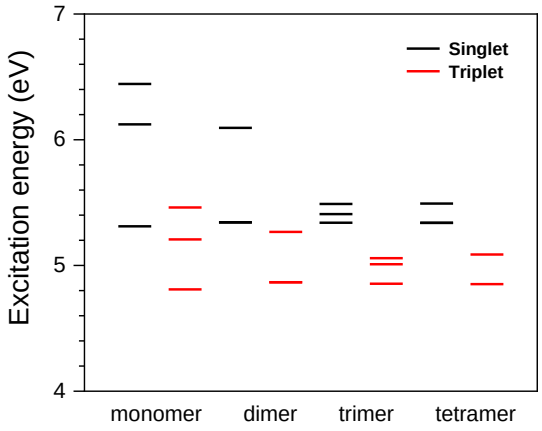

Figure S33. The excitation energy diagram of monomer, dimer, trimer, and tetramer of HA.

Table S5. Transition configurations of HA.

Aggregation state	Excited state	Excitation energy [eV]	Transition configuration
monomer	S_1	5.3113	H-3 → L (0.10045), H → L (0.65418)
	T_1	4.8096	H-3 → L (0.12340), H → L (0.62130)
	T_2	5.2072	H-3 → L (0.56695), H-2 → L (0.29135)
dimer	S_1	5.3421	H-5 →L (0.19220), H-1 → L (0.44753), H → L+1 (0.46109)
	T_1	4.8659	H-5 → L (0.23907), H-1 → L (0.41764), H → L+1 (0.43441)
	T_2	4.8669	H-5 → L+1 (0.24664), H-1 → L+1 (0.42598), H → L (0.42654)
	T_3	5.2671	H-4 → L+1 (0.27498), H-2 → L (0.24886)
trimer	S_1	5.3401	H-4 → L (0.56377), H-4 → L+1 (0.23695)
	T_1	4.8549	H-4 → L (0.53747), H-4 → L+1 (0.22394)
	T_2	5.0100	H-11 → L+2 (0.23667), H-1 → L+2 (0.53497)
	T_3	5.0579	H-6 → L+3 (0.12025), H-1 → L+3 (0.14486), H → L+3 (0.55195)
tetramer	S_1	5.339	H-12 → L+1 (0.14249)
	T_1	4.8518	H-11 → L (0.15232), H-11 → L+1 (0.10578), H-5 → L (0.33325), H-5 → L+1 (0.22698), H-5 → L+2 (0.12343), H-4 → L (0.23650), H-4 → L+1 (0.36511)
	T_2	4.8519	H-11 → L+1 (0.15766), H-5 → L+1 (0.35253), H-4 → L (0.34564), H-4 → L+2 (0.12787)
	T_3	5.0869	H-15 → L+3 (0.18977), H-8 → L+2 (0.16667), H-2 → L+2 (0.14694), H-1 → L+2 (0.37478)

References

1. Zhao, W.; Cheung, T. S.; Jiang, N.; Huang, W.; Lam, J. W. Y.; Zhang, X.; He, Z.; Tang, B. Z. Boosting the Efficiency of Organic Persistent Room-Temperature Phosphorescence by Intramolecular Triplet-Triplet Energy Transfer. *Nat. Commun.* **2019**, *10*, 1595.
2. Li, M.; Ling, K.; Shi, H.; Gan, N.; Song, L.; Cai, S.; Cheng, Z.; Gu, L.; Wang, X.; Ma, C.; Gu, M.; Wu, Q.; Bian, L.; Liu, M.; An, Z.; Ma, H.; Huang, W. Prolonging Ultralong Organic Phosphorescence Lifetime to 2.5 s through Confining Rotation in Molecular Rotor. *Adv. Opt. Mater.* **2019**, *7*, 1800820.
3. Bolton, O.; Lee, K.; Kim, H. J.; Lin, K. Y.; Kim, J. Activating Efficient Phosphorescence from Purely Organic Materials by Crystal Design. *Nat. Chem.* **2011**, *3*, 205-210.
4. Yuan, J.; Wang, S.; Ji, Y.; Chen, R.; Zhu, Q.; Wang, Y.; Zheng, C.; Tao, Y.; Fan, Q.; Huang, W. Invoking Ultralong Room Temperature Phosphorescence of Purely Organic Compounds through H-Aggregation Engineering. *Mater. Horiz.* **2019**, *6*, 1259-1264.
5. Cai, S.; Ma, H.; Shi, H.; Wang, H.; Wang, X.; Xiao, L.; Ye, W.; Huang, K.; Cao, X.; Gan, N.; Ma, C.; Gu, M.; Song, L.; Xu, H.; Tao, Y.; Zhang, C.; Yao, W.; An, Z.; Huang, W. Enabling Long-Lived Organic Room Temperature Phosphorescence in Polymers by Subunit Interlocking. *Nat. Commun.* **2019**, 10, 4247.
6. Mao, Z.; Yang, Z.; Xu, C.; Xie, Z.; Jiang, L.; Gu, F. L.; Zhao, J.; Zhang, Y.; Aldred, M. P.; Chi, Z. Two-Photon-Excited Ultralong Organic Room Temperature Phosphorescence by Dual-Channel Triplet Harvesting. *Chem. Sci.* **2019**, *10*, 7352-7357.
7. Xie, Y.; Ge, Y.; Peng, Q.; Li, C.; Li, Q.; Li, Z. How the Molecular Packing Affects the Room Temperature Phosphorescence in Pure Organic Compounds: Ingenious Molecular Design, Detailed Crystal Analysis, and Rational Theoretical Calculations. *Adv. Mater.* **2017**, *29*, 1606829.
8. Cai, S.; Shi, H.; Tian, D.; Ma, H.; Cheng, Z.; Wu, Q.; Gu, M.; Huang, L.; An, Z.; Peng, Q.; Huang, W. Enhancing Ultralong Organic Phosphorescence by Effective Π-Type Halogen Bonding. *Adv. Funct. Mater.* **2018**, *28*, 1705045.
9. Gu, L.; Shi, H.; Bian, L.; Gu, M.; Ling, K.; Wang, X.; Ma, H.; Cai, S.; Ning, W.; Fu, L.; Wang, H.; Wang, S.; Gao, Y.; Yao, W.; Huo, F.; Tao, Y.; An, Z.; Liu, X.; Huang, W. Colour-Tunable Ultra-Long Organic Phosphorescence of a Single-Component Molecular Crystal. *Nat. Photonics* **2019**, *13*, 406-411.
10. Zhou, Q.; Wang, Z.; Dou, X.; Wang, Y.; Liu, S.; Zhang, Y.; Yuan, W. Z. Emission Mechanism Understanding and Tunable Persistent Room Temperature Phosphorescence of Amorphous Nonaromatic Polymers. *Mater. Chem. Front.* **2019**, *3*, 257-264.